Positions of the phenyl hydrogens were held fixed during refinement. Isotropic thermal parameters for the methyl hydrogens were set at 1.2 times the initial equivalent isotropic thermal parameter of the methyl carbon and were not refined. Remaining hydrogen isotropic thermal parameters were refined. An extinction correction was applied. The absolute configuration was confirmed in the refinement. The value of η was 1.3 (3) with $\eta = +1$ indicating the proper absolute configuration and $\eta = -1$ the wrong choice. Structure solution details are included in the supplementary material. Standard atomic scattering factors were used.[28] Computer programs used are contained in the program package SHELXTL.[29]

Acknowledgment. We thank the American Cancer Society (CH-405), the Natural Sciences and Engineering Research Council of Canada, and Brigham Young University development funds for generous support. We thank Mrs. Kathryn M. Rollins for assistance with the manuscript.

Registry No. **1a**, 136721-70-5; **1b**, 136721-71-6; **2a**, 136721-72-7; **2c**, 136721-73-8; **3b**, 136721-74-9; **4a**(5′*R*), 136721-75-0; **4a**(5′*S*), 136721-76-1; **4c**(5′*R*), 136721-77-2; **4c**(5′*S*), 136721-78-3; **5b**(5′*R*), 136721-79-4; **5b**(5′*S*), 136721-80-7; **6a**(5′*R*), 136721-81-8; **6a**(5′*S*), 136721-82-9; **6c**(5′*R*), 136721-83-0; **6c**(5′*S*), 136721-84-1; **7a**(5′*R*), 136721-85-2; **7a**(5′*S*), 136721-86-3; **7b**(5′*R*), 136721-87-4; **7b**(5′*S*), 136721-88-5; (*R*,*R*)-**8a**, 136721-89-6; (*R*,*S*)-**8a**, 136779-77-6; (*S*,*R*)-**8a**, 136779-78-7; (*S*,*S*)-**8a**, 136779-79-8; **9a**(5′*R*), 136721-90-9; **9a**(5′*S*), 136721-91-0; **10a**(5′*R*), 136721-92-1; **10a**(5′*S*), 136721-93-2.

Supplementary Material Available: Tables 1S–5S containing a summary of the crystal data, structure determination details, atom positional and thermal parameters, bond lengths and angles, and important sugar torsion angles of **6a**(5′*R*) (6 pages). Ordering information is given on any current masthead page.

---

[28] *International Tables for X-Ray Crystallography*; Ibers, J. A., Hamilton, W. C., Eds.; Kynoch Press: Birmingham, England, 1974; Vol. 4, p 99.

[29] Sheldrick, G. M. *SHELXTL. An Integrated System for Solving, Refining, and Displaying Crystal Structures from Diffraction Data*; University of Göttingen: Federal Republic of Germany, 1983; 4th revision.

[30] Sheldrick, G. M. *SHELXTL PLUS*. Siemens Analytical X-ray Instruments, Inc., Madison, WI, 1990.

Comparative Structural Studies of [3.1.0]-Fused 2′,3′-Modified β-D-Nucleosides by X-ray Crystallography, NMR Spectroscopy, and Molecular Mechanics Calculations

Leo H. Koole,[†] Stephen Neidle,[‡] Mark D. Crawford,[‡] Alexander A. Krayevski,[§]
Galyna V. Gurskaya,[§] Anders Sandström,[†] Jin-Chang Wu,[†] Weimin Tong,[†] and
Jyoti Chattopadhyaya*[,†]

Department of Bioorganic Chemistry, Box 581, Biomedical Center, University of Uppsala, S-75 123 Uppsala, Sweden, Cancer Research Campaign Biomolecular Structure Unit, The Institute of Cancer Research, Sutton, Surrey SM2 5NG, United Kingdom, and Institute of Molecular Biology, Academy of Sciences of USSR, Vavilov str. 32, 117984 Moskva B-334, USSR

Received May 9, 1991

A structural study is reported on the [3.1.0]-fused nucleosides 2′,3′-dideoxy-2′,3′-α-methyleneuridine (**1**), 1-(2′,3′-dideoxy-2′,3′-epimino-β-D-ribofuranosyl)uracil (**2**), 1-(2′,3′-dideoxy-2′,3′-epithio-β-D-ribofuranosyl)uracil (**3**), 2′,3′-*O*-anhydroadenosine (**4**), 1-(2′,3′-dideoxy-2′,3′-epithio-β-D-lyxofuranosyl)uracil (**5**), 1-(2′,3′-*O*-anhydro-β-D-lyxofuranosyl)uracil (**6**), 9-(2′,3′-*O*-anhydro-β-D-lyxofuranosyl)adenine (**7**), and 1-(2′,3′-*O*-anhydro-β-D-lyxofuranosyl)thymine (**8**). Note that compounds **1–4** have the three-membered fused ring in the exo orientation (α-face) and compounds **5–8** have the three-membered fused ring in the endo orientation (β-face). The X-ray crystal structure of compounds **1** and **4** show that both systems have an almost planar furanoid ring. Comparisons are made with the crystal structures of the native nucleosides (i.e., uridine and adenosine, respectively). This shows that the cyclopropane unit in **1** and the epoxide ring in **4** have virtually the same impact on the furanoid conformation, i.e., flattening of the furanoid ring is in both cases accompanied by shortening of the bonds C1′–C2′ and C2′–C3′ by ca. 0.03 Å, and expansion of the bond angles C1′–C2′–C3′ and C2′–C3′–C4′ by 5–6°. Comparison of the crystal structures of [3.1.0]-fused nucleosides **1** and **4** with three [3.3.0]-fused nucleosides from the literature with a flattened sugar ring showed that C2′-C3′ [3.1.0]-fused nucleosides display subtle structural differences, despite the fact that rotation around C2′–C3′ is blocked. Secondly, a ^{1}H NMR conformational study on compounds **1–8** is reported. Thirdly, we have investigated whether molecular mechanics calculations (using Allinger's MM2-87 method as provided in the CHEM3D package) can be used to study the conformational properties of systems **1–8**. In this respect, the structural data on **1**, **4**, and **8** were used to evaluate the performance of the MM2-87 method. It turns out that the molecular mechanics calculations lead to a fairly accurate picture of the structure of the modified sugar ring, while the calculated values for the torsion angles γ and χ frequently show disparities with respect to the experimental data. It is put forward that this will be partly due to the fact that intermolecular interactions in the crystal (hydrogen bonding and base stacking) have an impact on the molecular conformation; this effect is not mimicked in our calculations.

Introduction

The search for potential agents against the human immunodeficiency virus type I (HIV I) has greatly stimulated studies on structurally modified nucleosides in the last years.[1] Most of this work has been devoted to nucleoside analogues lacking the 3′-hydroxyl group. Several members of this family of compounds have shown antiretroviral

---

[†] University of Uppsala.

[‡] The Institute of Cancer Research.

[§] Academy of Sciences of USSR.

[1] For an excellent review, see: Mitsuya, H.; Yarchoan, R.; Broder, S. *Science* **1990**, *249*, 1533.

0022-3263/91/1956-6884$02.50/0 © 1991 American Chemical Society

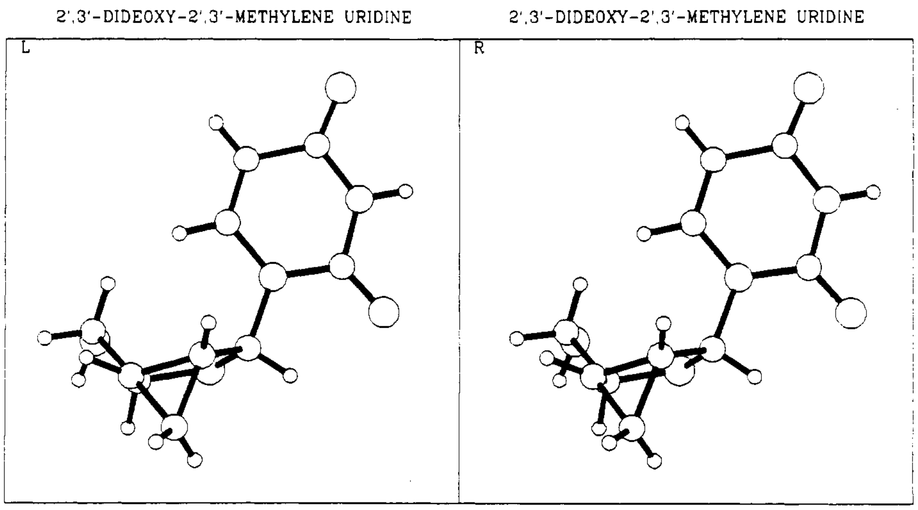

Figure 1. Stereoview of the crystal structure of compound 1. The virtually flat structure of the furanoid ring is clearly visible.

activity, e.g., 3′-α-azido-2′,3′-dideoxythymidine (AZT),[2] 2′,3′-dideoxycytidine (ddC),[3] 2′,3′-dideoxyinosine (ddI),[4] 2′,3′-dideoxyadenosine (ddA),[5] 3′-α-fluoro-2′,3′-dideoxythymidine (FLT),[6] and 2′,3′-didehydro-2′,3′-dideoxythymidine (D4T).[7] One of our research objectives in the past years has been to prepare [3.1.0]-fused 2′,3′-modified nucleosides and to perform in vitro tests on their anti-HIV I potential. This work has led to a variety of novel [3.1.0]-fused 2′,3′-modified β-D-nucleoside analogues,[8] none of which, however, showed promising HIV-I inhibitory effects. Recent work by Krayevski et al. showed that 5′-triphosphate derivatives of 2′,3′-*O*-riboanhydroadenosine, 2′,3′-*O*-lyxoanydro adenosine, and 2′,3′-*O*-lyxoanhydro thymidine effectively inhibit the action of several DNA polymerases, including virus reverse transcriptases.[9]

In this paper, we report on the structural properties of eight [3.1.0]-fused 2′,3′-modified nucleosides: i.e., 2′,3′-dideoxy-2′,3′-α-methyleneuridine (**1**), 1-(2′,3′-dideoxy-2′,3′-epimino-β-D-ribofuranosyl)uracil (**2**), 1-(2′,3′-dideoxy-2′,3′-epithio-β-D-ribofuranosyl)uracil (**3**), 2′,3′-*O*-anhydroadenosine (**4**), 1-(2′,3′-dideoxy-2′,3′-epithio-β-D-lyxofuranosyl)uracil (**5**), 1-(2′,3′-*O*-anhydro-β-D-lyxofuranosyl)uracil (**6**), 9-(2′,3′-*O*-anhydro-β-D-lyxofuranosyl)adenine (**7**), and 1-(2′,3′-*O*-anhydro-β-D-lyxofuranosyl)thymine (**8**).[10] Note that compounds **1**–**4** have

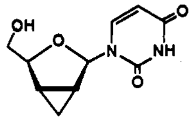

1

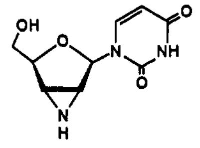

2

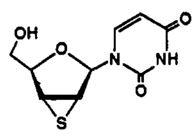

3

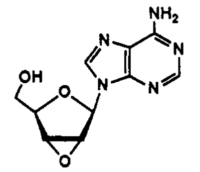

4

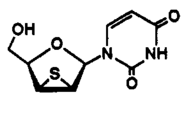

5

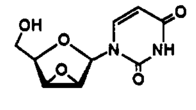

6

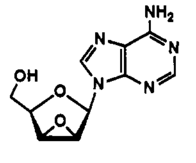

7

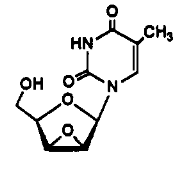

8

the three-membered fused ring in the exo orientation (α-face) and compounds **5**–**8** have the three-membered fused ring in the endo orientation (β-face). We have attempted to understand the impact of the three-membered fused rings on the conformation properties of **1**–**8**, used different techniques (X-ray crystallography, high-field (500-MHz)

---

(2) (a) Kim, C.-H.; Marquez, V. E.; Broder, S.; Mitsuya, H.: Driscoll, J. *J. Med. Chem.* **1987**, *30*, 862. (b) Mitsuya, H.; Weinhold, K. J.; Furman, P. A.; St. Clair, M. H.; Nusinoff Lehrman, S.; Gallo, R. C.; Bolognesi, D.: Barry, D. W.; Broder, S. *Proc. Natl. Acad. Sci. U.S.A.* **1985**, *82*, 7096.

(3) (a) Mitsuya, H.; Broder, S. *Proc. Natl. Acad. Sci., U.S.A.* **1986**, *87*, 1911. (b) Mitsuya, H.; Broder, S. *Nature (London)* **1987**, *325*, 773. (c) Yarchoan, R.; Perno, C. F.; Thomas, R. V.; Klecker, R. W.; Allain, R. J.; McAtee, N.; Fischl, M. A.; Dubinsky, R.; McNeely, M. C.; Mitsuya, H.; Pluda, J. M.; Lawley, T. J.; Leuther, M.; Safai, B.; Collins, J. M.; Myers, C. E.; Broder, S. *Lancet* **1988**, *1*, 76.

(4) (a) Yarchoan, R.; Mitsuya, H.; Thomas, R. V.; Pluda, J. M.; Hartman, N. R.; Perno, C.-F.; Marczyk, K. C.; Allain, J. P.; Johns, D. G.; Broder, S. *Science* **1989**, *245*, 412. (b) McGowan, J. J.; Tomaszewski, J. E.; Cradock, J.; Hoth, D.; Grieskaber, C. K.; Broder, S.; Mitsuya, H. *Rev. Infect. Dis.* **1990**, *12* (*Suppl.*), 513 and other references in this issue, which was devoted entirely to clinical use of ddI.

(5) (a) Perno, C.-F.; Yarchoan, R.; Cooney, D. A.; Hartman, N. R.; Gartner, S.; Popovic, M.; Hao, Z.; Gerrard, T. L.; Wilson, Y. A.; Johns, D. G.; Broder, S. *J. Exp. Med.* **1988**, *168*, 1111. (b) Zimmerman, T. P.; Mahony, W. B.; Prus, K. L. *J. Biol. Chem.* **1987**, *262*, 5748.

(6) (a) Datema, R.; Remaud, G.; Bazin, H.; Chattopadhyaya, J. *Biochemical Pharmacology* **1989**, *38*, 109. (b) Lin, T. S.; Schinazi, R. F.; Prusoff, W. H. *Biochem. Pharmacol.* **1987**, *17*, 2713.

(7) (a) Hamamoto, Y.; Nakashima, H.; Matsui, T.; Matsuda, A.; Ueda, T.; Yamamoto, N. *Antimicrob. Agents Chemother.* **1987**, *31*, 907. (b) Balzarini, J. *Mol. Pharmacol.* **1987**, *32*, 162.

(8) (a) Wu, J.-C.; Chattopadhyaya, J. *Tetrahedron* **1990**, *46*, 2587. (b) Wu, J.-C.; Chattopadhyaya, J. *Tetrahedron* **1989**, *45*, 4507. Tong, W.; Wu, J.-C.; Chattopadhyaya, J. *Tetrahedron* **1990**, *46*, 3037. (c) Bazin, H.; Chattopadhyaya, J. *Synthesis* **1985**, 1108. Nyilas, A.; Chattopadhyaya, J. *Synthesis* **1986**, 196. (d) Codington, J. F.; Fecher, R.; Fox, J. J. *J. Org. Chem.* **1962**, *27*, 163. Vial, J.-M.; Johansson, N. G.; Vrang, L.; Chattopadhyaya, J. *Antiviral Chem. Chemother.* **1990**, *1(3)*, 183.

(9) (a) Krayevski, A. A.; Kukhanova, M. K.; Atrazhev, A. M.; Dyatkina, N. B.; Papchikhin, A. V.; Chidgeavadze, Z. G.; Beabealasvilli, R. Sh. *Nucleosides Nucleotides* **1988**, *7*, 613. (b) Chidgeavadze, Z. G.; Beabealashvilli, R. Sh.; Rosovskaya, T. A.; Atrazhev, A. M.; Tarussova, N. B.; Dyatkina, N. B.; Kukhanova, M. K.; Krayevski, A. A. *Mol. Biol. Moscow* **1989**, *23*, 1732.

(10) Syntheses of compounds **1**–**8** have been published. Compound: **1**, ref 8a; **2**, ref 8b; **3** and **5**, ref 8c; **4** and **7**, ref 8d; **6** and **8**, ref 8e.

^{1}H NMR spectroscopy, and molecular mechanics calculations) in an integrated fashion.

Results and Discussion

X-ray Crystal Structure of Compounds 1 and 4. The crystal structure of 1 is shown in Figure 1. The positional parameters are compiled in Table I, and Table II summarizes the most important conformational characteristics. The most striking feature is that the furanose moiety is approximately coplanar. The maximum puckering amplitude (ν_m) amounts to only 8.8°; the phase angle of pseudorotation (*P*) is 86.7°, corresponding to an O4′-endo pucker.[11] The cyclopropane ring in 1 is inclined at an angle of 72.5 (3)° to the mean plane of the furanose ring, pointing in the exo orientation. The cyclopropane ring is an almost exact equilateral triangle, the bond lengths C2′–C3′, C2′–C23, and C3′–C23 are 1.496 (4), 1.469 (4), and 1.499 (4) Å, respectively. The conformation about the glycosidic bond is anti, with a value of −106.9 (4)° for χ[C2-N1-C1′-O4′].[12,13] The conformation around the C4′–C5′ bond is γ^t (i.e., trans orientation of O5′ and C3′) with γ[O5′-C5′-C4′-C3′] = −174.7 (4)°. The fusion of the cyclopropane ring to the ribose group does appear to have induced several changes in bond geometry in its vicinity. The impact of the cyclopropane ring becomes more clear via a comparison with the X-ray crystal structure of uridine, which shows two independent molecules (a and b) in the unit cell.[14] Table II serves to facilitate this comparison. The furanoid ring in 1 is very much flattened in comparison with both uridine structures; compare the ν_m values of 8.8° in 1 with 40.6° and 41.6° in uridine, Table II. The bonds C1′–C2′ and C2′–C3′ are shortened by approximately 0.03 Å in 1, while the bonds C3′–C4′, C4′–O4′, and C1′–O4′ have almost the same length. Also, the bond lengths C4′–C5′ and C1′–N1 do not differ for 1 and uridine. As expected, the endocyclic furanose bond angles show appreciable differences: the angles C1′–C2′–C3′ and C2′–C3′–C4′ are increased by 5–6° in 1. These bond angle expansions are the consequence of the flattening of the five-membered ring. the glycosidic torsion angle χ[C2–N1–C1′–O4′] is approximately 50° larger in 1 than in both uridine structures; molecular mechanics calculations indicate that this conformation is accessible because of the flattened furanose ring (vide infra). Clear discrepancies between 1 and uridine are also noted for the torsion angle about the exocyclic C4′–C5′ bond (γ^t in 1, γ^+ in uridine). It is not evident, however, that these differences in γ are directly caused by the cyclopropane moiety; the conformation around C4′–C5′ and/or C5′–O5′ may very well be determined by intermolecular hydrogen bonding in the crystal lattice.

The crystal structure of compound 4 shows two independent molecules (**4a** and **4b**) in the unit cell. Both structures are presented in Figure 2. Positional parameters of **4a,b** are listed in Table III. Important structural features of **4a,b** are also summarized in Table II. Structures **4a** and **4b** differ with respect to the conformation around the glycosidic C1′–N9 bond, which is high syn for **4a** and anti for **4b**. Both structures show an almost flat furanose ring, the maximum puckering amplitudes for **4a** and **4b** are only 8.1° and 9.3°, respectively.[15] The phase angles of pseudorotation are 123.0° (approximately C1′-exo pucker) for **4a** and 249.8° (approximately C4′-endo-O4′-exo pucker) for **4b**. The epoxide ring in both molecules is an almost equilateral triangle with C2′–C3′, C2′–O23, and C3′–O23 bond distances of 1.456 (4), 1.477 (4), and 1.438 (4) Å, respectively, in **4a** and 1.453 (4), 1.443 (4), and 1.443 (4) Å, respectively, in **4b**.

Table I. Positional Parameters and Their Estimated Standard Deviations for Compound 1[a]

atom	*x*	*y*	*z*	*B* (Å^2)
O(2)	0.0334 (3)	0.0942 (2)	1.0720 (1)	5.01 (5)
O(4)	−0.0268 (2)	0.1826 (2)	0.7774 (1)	3.44 (4)
O(4′)	−0.1422 (2)	0.4690 (2)	1.1484 (1)	2.93 (3)
O(5′)	−0.4299 (2)	0.6807 (2)	1.1132 (1)	2.93 (4)
N(1)	0.0036 (3)	0.3536 (2)	1.0265 (1)	2.64 (4)
N(3)	0.0021 (3)	0.1447 (2)	0.9252 (1)	2.77 (4)
C(1′)	0.0152 (3)	0.4159 (3)	1.1185 (1)	2.73 (4)
C(2)	0.0134 (3)	0.1903 (3)	1.0130 (1)	2.96 (5)
C(2′)	0.1312 (3)	0.5541 (3)	1.1256 (2)	3.08 (5)
C(3′)	0.0311 (3)	0.6960 (3)	1.1527 (2)	3.11 (5)
C(4)	−0.0192 (3)	0.2420 (3)	0.8525 (2)	2.60 (4)
C(4′)	−0.1452 (3)	0.6403 (3)	1.1623 (2)	2.61 (5)
C(5)	−0.0298 (4)	0.4086 (3)	0.8723 (2)	3.05 (5)
C(5′)	−0.2607 (3)	0.7228 (3)	1.0988 (2)	3.31 (5)
C(6)	−0.0180 (3)	0.4571 (3)	0.9565 (1)	2.92 (5)
C(*)	0.1504 (4)	0.6225 (4)	1.2169 (2)	4.08 (6)
H(1′)	0.047 (3)	0.323 (3)	1.154 (2)	4.08 (6)*
H(3)	0.017 (4)	0.037 (3)	0.914 (2)	2.6 (6)*
H(4′)	−0.191 (3)	0.653 (3)	1.226 (1)	0.3 (5)*
HO(5′)	−0.454 (3)	0.716 (3)	1.166 (2)	1.6 (6)*
H(5)	−0.041 (3)	0.478 (3)	0.824 (2)	1.6 (6)*
H(6)	−0.013 (3)	0.572 (3)	0.971 (1)	0.8 (5)*
H(5′)	−0.242 (3)	0.842 (3)	1.107 (2)	1.4 (6)*
H(5″)	−0.239 (3)	0.692 (3)	1.036 (2)	2.0 (6)*
H(*1)	0.110 (3)	0.565 (3)	1.261 (2)	2.1 (6)*
H(*2)	0.246 (4)	0.687 (4)	1.233 (2)	2.9 (7)*
H(2′)	0.220 (3)	0.561 (3)	1.084 (2)	1.3 (6)*
H(3′)	0.053 (3)	0.805 (3)	1.129 (1)	0.9 (5)*

[a] Starred atoms were refined isotropically. Numbers in parentheses are estimated standard deviations in the least significant digits. Anisotropically refined atoms are given in the form of the isotropic equivalent thermal parameter defined as: $(4/3) * (2a*B(1,1) + b2*B(2,2) + c2*B(3,3) + ab(\cos\gamma)*B(1,2) + ac(\cos\beta)*B(1,3) + bc(\cos\alpha)*B(2,3))$.

The structural effects of the epoxide ring in **4a,b** were again evaluated by means of a comparison with the crystal structure of (unmodified) adenosine (Table II).[16] Comparison of the ν_m values of **4a,b** and adenosine (36.8°) clearly demonstrates the flattening of the furanoid ring in **4a,b**. The C1′–C2′ and C2′–C3′ bonds are shortened by approximately 0.03 and 0.07 Å, respectively, in **4a,b**, while the other three bond distances of the furanoid ring are grossly similar. Note that this closely resembles the observations on compound 1. The endocyclic bond angles C1′–C2′–C3′ and C2′–C3′–C4′ in **4a,b** are found to be expanded by 5–6°, and the other three endocyclic bond angles are very similar in **4a,b** and adenosine, which is another analogy between structures 1 (vide supra) and **4a,b**. *Our analyses on 1 and 4 thus show for the first time that introduction of a C2′/C3′ α-cyclopropane ring or a C2′/C3′ α-epoxide ring has essentially the same effect: shortening of the bonds C1′–C2′ and C2′–C3′ and expansion of the bond angles C1′–C2′–C3′ and C2′–C3′–C4′. The three-*

---

[11] The pseudorotation concept was used throughout this work to describe conformations of furanose rings. See: Altona, C.; Sundaralingam, M. *J. Am. Chem. Soc.* **1972**, *94*, 8205.

[12] van Roey, P.; Salemo, J. M.; Duax, W. L.; Chu, C. K.; Ahn, M. K.; Schinazi, R. F. *J. Am. Chem. Soc.* **1988**, *110*, 2277.

[13] (a) Neidle, S.; Kaye, A.; Reese, C. B. *Acta Crystallogr.* **1990**, *B46*, 426. (b) Birnbaum, G. I.; Lin, T.-S.; Prusoff, W. H. *Biochem. Biophys. Res. Commun.* **1988**, *151*, 608.

[14] Green, E. A.; Rosenstein, R. D.; Shiono, R.; Abraham. D. J.; Trus, B. L.; Marsh, R. E. *Acta Crystallogr.* **1975**, B31, 102.

[15] It is well-known that adenosine derivatives with a flattened furanose ring tend to adopt a *syn*-type conformation which is stabilized through a N3⋯H-O5′ hydrogen bond. See, e.g.: (a) Ikehara, M.; Uesugi, S.; Kaneko, M. *Nucl. Acid. Chem.* **1978**, 837. (b) Koole, L. H.; de Boer, H.; de Haan, J. W.; Haasnoot, C. A. G.; van Dael, P.; Buck, H. M. *J. Chem. Soc., Chem. Commun.* **1986**, 362. See also ref 18(b).

[16] Lai, T. F.; Marsh, R. E. *Acta Crystallogr.* **1972**, *B28*, 1982.

Table II. Major Geometric and Conformation Features of the Crystal Structures of Compounds 1 and 4 (esds are in Parentheses. X* = C(H_2) in 1 and O in 4. Structural Data on Uridine[14] and Adenosine[16] Are Also Given to Facilitate Comparisons)

		uridine		compd 4		
	compd 1	molec a	molec b	molec a	molec b	adenosine
(a) bond lengths						
C1′–C2′	1.496 (4)	1.528 (4)	1.533 (4)	1.482 (4)	1.501 (4)	1.530 (3)
C2′–C3′	1.497 (4)	1.527 (4)	1.525 (4)	1.456 (4)	1.453 (4)	1.528 (3)
C2′–X*	1.469 (4)			1.477 (4)	1.443 (4)	
C3′–X*	1.499 (4)			1.438 (4)	1.443 (4)	
(b) bond angles						
C1′–C2′–C3′	107.1 (2)	100.4 (3)	100.6 (3)	108.3 (3)	106.5 (3)	101.4 (2)
C2′–C3′–C4′	107.0 (4)	102.1 (3)	101.2 (3)	107.4 (3)	108.8 (3)	102.7 (2)
C1′–C2′–X*	115.4 (2)			108.8 (3)	109.2 (3)	
C2′–C3′–X*	59.9 (2)			61.4 (3)	59.3 (3)	
C3′–C2′–X*	60.1 (2)			58.7 (3)	60.6 (3)	
C2′–X*–C3′	60.2 (2)			59.9 (3)	60.1 (3)	
X*–C3′–C4′	114.9 (2)			111.8 (3)	113.1 (3)	
(c) torsion angles						
C4′–O4′–C1′–C2′ (ν_0)	8.7 (4)	10.5 (3)	3.4 (3)	–7.9 (4)	7.4 (4)	7.4 (4)
O4′–C1′–C2′–C3′ (ν_1)	–5.4 (4)	–31.4 (3)	–27.9 (3)	7.5 (4)	–2.5 (4)	–27.3 (4)
C1′–C2′–C3′–C4′ (ν_2)	0.5 (4)	39.5 (3)	40.4 (3)	–4.4 (4)	–3.2 (4)	35.7 (4)
C2′–C3′–C4′–O4′ (ν_3)	4.6 (4)	–34.6 (3)	–39.5 (3)	–0.3 (4)	7.5 (4)	–32.5 (4)
C3′–C4′–O4′–C1′ (ν_4)	–8.3 (4)	15.3 (3)	22.8 (3)	5.2 (4)	–9.4 (4)	16.0 (4)
O4′–C1′–N1–C2 (χ)	–106.9 (4)	–161.7 (3)	–155.7 (3)			
O4′–C1′–N9–C4 (χ)				56.8 (4)	170.8 (4)	–9.9 (4)
O5′–C5′–C4′–C3′ (γ)	–174.7 (4)	45.9 (3)	39.6 (3)	42.9 (4)	44.0 (4)	177.0 (4)
O5′–C5′–C4′–O4′	65.9	–72.9 (3)	–77.7 (3)	–75.9 (4)	–75.0 (4)	
phase angle of pseudorotation	6.7	13.4	14.0	123.0	249.8	7.2
maximum puckering amplitude	8.8	40.6	41.6	8.1	9.3	36.8
sugar pucker description	O4′-exo	C3′-endo	C3′-endo	C1′-exo	C4′-endo	C4′-endo

Structure 4a

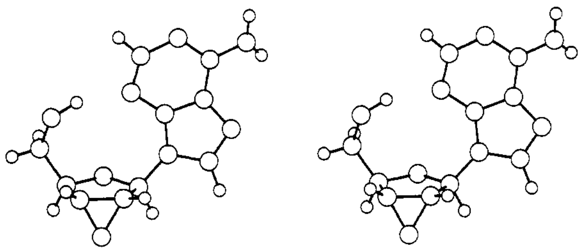

Structure 4 b

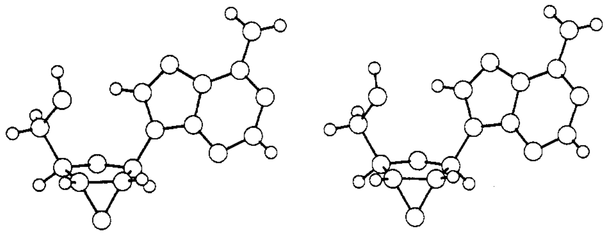

Figure 2. Stereoviews of the two crystallographically independent molecules in the crystal structure of compound 4. Structure **4a** shows *syn* orientation of the adenine base, which is probably stabilized via the intramolecular O5′-H···N3 hydrogen bond. In **4b**, the adenine ring is in the *anti* domain. The furanoid rings in **4a** and **4b** are almost completely planar.

membered ring is almost equilateral in both cases.

It is also of interest to compare the results on 1 and 4 with the X-ray crystal structure of compound 8, which was published recently.[17] Surprisingly, the furanoid ring in 8 was found to adopt an O4′-endo *puckered* conformation. The pseudorotational parameters of the two crystallographically independent molecules (**8a** and **8b**) were found to be $P = 98.9°$, $\nu_m = 29.2°$ for **8a**, and $P = 97.6°$, $\nu_m = 33.1°$, for **8b**. Alternatively stated, the six-membered ring C1′–C2′–O23–C3′–C4′–O4′ resides in a boat conformation for compound 8, but in a half-boat (chaise lounge) conformation for structures 1 and 4. Further inspection of the crystal structures **8a** and **8b** shows that the O4′-endo conformation of the furanoid ring has resulted in a relatively remote location of the thymine base and the CH_2OH group on C4′. Conversely, a similar conformation for the structures 1 and 4 would have resulted in a *close* location of the uridine and the CH_2OH group. This may explain why flat furanoid rings are found for 1 and 4 (α-orientation of the three-membered ring) versus a puckered furanoid ring in the case of 8 (β-orientation of the epoxy ring). Apparently, the puckered structure is intrinsically preferred by a furanose ring in which a three-membered ring is fused to C2′ and C3′. It is the location of the bulky uridine base and the CH_2OH group on the β-side of the furanoid ring that prevents puckering in the case of structures 1 and 4.

The crystal structures of 1 and 4 provide two novel examples of a virtually planar furanoid ring in nucleosides or nucleotides. To the best of our knowledge, this was observed only for [3.3.0]-fused 2′,3′-*O*-isopropylideneadenosine (9),[18a] 8-bromo-2′,3′-*O*-isopropylideneadenosine (10),[18b] and cytidine 2′,3′-*O*-phosphate (11).[18c,19] Coexistence of a planar and a puckered ribofuranose ring was found in the case of 2′,3′-*O*-isopropylideneadenosine (9)

---

[17] Gurskaya, G. V.; Bochkarev, A. V.; Zdanov, A. S.; Papchikhin, A. V.; Purygin, P. P.; Krayevski, A. A. *FEBS Lett.* **1990**, *265*, 63.

[18] (a) Sprang, S.; Rohrer, D. C.; Sundaralingam, M. *Acta Crystallogr.* **1978**, *B34*, 2803. (b) Fujii, S.; Fujiwara, T.; Komita, K. *Nucl. Acids Res.* **1976**, *3*, 1985. (c) Coulter, C. L. *J. Am. Chem. Soc.* **1973**, *95*, 570.

[19] Relevant geometric data on these structures are as follows: (i) 2′,3′-*O*-isopropylidene adenosine (flat molecule, ref 18a) $\nu_0 = -0.6°$, $\nu_1 = -2.0°$, $\nu_2 = 3.5°$, $\nu_3 = -3.9°$, $\nu_4 = 2.8°$, $P = 26.2°$, $\nu_m = 4.0°$, $\chi = -169.5°$ (anti); (ii) 8-bromo-2′,3′-*O*-isopropylidene adenosine (flat molecule, ref 18b) $\nu_0 = -2.6°$, $\nu_1 = 2.1°$, $\nu_2 = -1.0°$, $\nu_3 = -0.3°$, $\nu_4 = 1.8°$, $P = 114.4°$, $\nu_m = 2.5°$, $\chi = 72°$ (*syn*); (iii) sodium β-cytidine-2′,3′-cyclic phosphate (ref 18c) $\nu_0 = 1.9°$, $\nu_1 = -0.7°$, $\nu_2 = -0.7°$, $\nu_3 = 1.8°$, $\nu_4 = -2.3°$, $P = 252.2°$, $\nu_m = 2.3°$, $\chi = 74.5°$ (*syn*).

Table III. Positional Parameters and Their Estimated Standard Deviations for Compound 4[a]

atom	*x*	*y*	*z*	*B* (A2)
N1A	0.7913 (8)	0.4051 (5)	−0.0018 (2)	3.19 (7)
C2A	0.6780 (9)	0.4861 (6)	0.0645 (3)	3.18 (8)
N3A	0.5135 (7)	0.4123 (5)	0.1138 (2)	3.00 (7)
C4A	0.4481 (9)	0.2281 (6)	0.0920 (2)	2.70 (8)
C5A	0.5355 (9)	0.1288 (6)	0.0233 (3)	2.92 (8)
C6A	0.7096 (9)	0.2234 (6)	−0.0248 (2)	2.77 (8)
N7A	0.4283 (9)	−0.0567 (5)	0.0178 (2)	3.66 (8)
C8A	0.292 (1)	−0.0710 (7)	0.0832 (3)	3.9 (1)
N9A	0.2931 (8)	0.0977 (5)	0.1309 (2)	3.01 (7)
NA	0.8165 (8)	0.1413 (6)	−0.0901 (2)	3.64 (8)
C1′A	0.193 (1)	0.1054 (6)	0.2127 (3)	3.32 (8)
C2′A	0.409 (1)	0.1050 (8)	0.2873 (3)	4.3 (1)
O23A	0.274 (1)	0.0695 (6)	0.3638 (2)	5.51 (9)
C3′A	0.374 (1)	0.2634 (8)	0.3433 (3)	3.9 (1)
C4′A	0.101 (1)	0.3739 (7)	0.2996 (3)	3.8 (1)
O4′A	0.0277 (7)	0.2770 (5)	0.2190 (2)	3.97 (6)
C5′A	0.154 (1)	0.5866 (8)	0.2845 (3)	4.8 (1)
O5′A	0.4095 (8)	0.6235 (5)	0.2558 (2)	4.91 (8)
N1B	0.217	0.352	0.813	3.00 (7)
C2B	0.332 (1)	0.2710 (6)	0.7487 (3)	3.11 (8)
N3B	0.5052 (8)	0.3472 (5)	0.6995 (2)	2.87 (7)
C4B	0.5686 (8)	0.5310 (6)	0.7238 (2)	2.49 (7)
C5B	0.4737 (9)	0.6301 (6)	0.7916 (2)	2.65 (8)
C6B	0.2915 (9)	0.5336 (6)	0.8372 (2)	2.69 (8)
N7B	0.5840 (8)	0.8152 (5)	0.7978 (2)	3.29 (7)
C8B	0.735 (1)	0.8261 (6)	0.7355 (3)	3.30 (9)
N9B	0.7326 (7)	0.6588 (5)	0.6884 (2)	2.60 (6)
NB	0.1842 (8)	0.6165 (5)	0.9029 (2)	3.33 (7)
C1′B	0.8860 (8)	0.6179 (6)	0.6154 (2)	2.65 (7)
C2′B	0.691 (1)	0.5996 (6)	0.5348 (3)	3.19 (8)
O23B	0.8502 (8)	0.5544 (4)	0.4662 (2)	4.05 (7)
C3′B	0.761 (1)	0.7541 (6)	0.4800 (3)	3.30 (9)
C4′B	0.980 (1)	0.8721 (6)	0.5260 (3)	3.15 (8)
O4′B	1.0648 (6)	0.7699 (4)	0.6047 (2)	3.17 (6)
C5′B	0.888 (1)	1.0778 (7)	0.5421 (3)	3.55 (9)
O5′B	0.0178 (7)	1.0774 (5)	0.5697 (2)	4.43 (7)
HC2A	0.74 (1)	0.618 (8)	0.075 (4)	3 (1)*
HC8A	0.18 (1)	−0.195 (9)	0.099 (4)	3 (1)*
H1NA	0.70 (1)	0.054 (9)	−0.109 (4)	4 (1)*
H2NA	0.97 (1)	0.205 (9)	−0.115 (4)	4 (1)*
HC1′A	0.07 (1)	−0.02 (1)	0.218 (4)	4 (1)*
HC2A′	0.61 (1)	0.018 (9)	0.289 (4)	3 (1)*
HC3′A	0.53 (1)	0.325 (9)	0.379 (4)	3 (1)*
HC4′A	−0.06 (1)	0.355 (9)	0.335 (4)	4 (1)*
H1C5′A	0.15 (1)	0.66 (1)	0.338 (4)	5 (2)*
H2C5′A	−0.00 (1)	0.64 (1)	0.241 (4)	4 (1)*
HO5A′	0.46 (1)	0.58 (1)	0.201 (4)	4 (1)*
HC2B	0.27 (1)	0.15 (1)	0.734 (4)	3 (1)*
HC8B	0.84 (1)	0.94 (1)	0.722 (4)	3 (1)*
H1NB	0.07 (1)	0.530 (9)	0.934 (4)	3 (1)*
H2NB	0.24 (1)	0.75 (1)	0.914 (4)	4 (1)*
HC1′B	0.99 (1)	0.507 (9)	0.632 (4)	3 (1)*
HC2′B	0.52 (1)	0.529 (9)	0.534 (4)	3 (1)*
HC3′B	0.62 (1)	0.79 (1)	0.426 (4)	4 (1)*
HC4′B	1.15 (1)	0.906 (9)	0.493 (4)	3 (1)*
H1C5′B	0.89 (1)	1.154 (9)	0.489 (4)	4 (1)*
H2C5′B	1.03 (1)	1.140 (9)	0.587 (4)	4 (1)*
HO5′B	0.61 (1)	1.187 (9)	0.612 (4)	4 (1)*

[a] Starred atoms were refined isotropically. Numbers in parentheses are estimated standard deviations in the least significant digits. Anisotropically refined atoms are given in the form of the isotropic equivalent thermal parameter defined as follows: $(4/3)*(2a*B(1,1) + b2*B(2,2) + c2*B(3,3) + ab(\cos \delta)*B(1,2) + ac(\cos \beta)*B(1,3) + bc(\cos \alpha)*B(2,3))$.

and 8-bromo-2′,3′-*O*-isopropylideneadensine (**10**). A planar furanose ring may be regarded as a intermediate between the standard C2′-endo and C3′-endo puckered conformations.[20] We have plotted the available data on *P* and χ for the present set of nucleosides with a flattened furanoid ring (Figure 3). Surprisingly, a whole range of *P* values appears to be accessible for this strained class of [3.1.0]-fused and [3.3.0]-fused nucleosides. Apparently, these subtle changes of *P* values arise due to small changes of endocyclic torsions which are most probably modulated due to the nonbonded interactions (such as van der Waals/electrostatic) with the endocyclic heteroatoms in the crystal lattice. It should be remembered, however, that *P* is quite sensitive to relatively small changes in the furanoid conformation, e.g., a change from slight O4′-exo to slight O4′-endo will shift *P* from 90° to 270°. Although all six data points are found virtually on a straight line we see no rationale for a linear relationship between *P* and χ. It seems doubtful whether slight conformational changes leading to relatively large changes in *P* have to be accompanied by a rotation around the glycosidic bond.

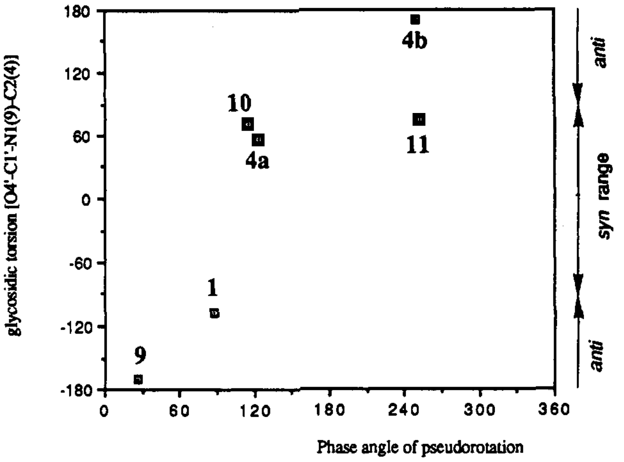

Figure 3. Plot of the glycosidic torsion angle χ [O4′–C1′–N1(9)–C2(4)] against the phase angle for pseudorotation *P* for the present set of nucleosides and nucleotides with a flattened sugar ring. Data points marked **1**, **4a**, and **4b** refer to the crystal structures presented in this work. Data points marked **9**, **10**, and **11** refer to the crystal structures of 2′,3′-*O*-isopropylideneadenosine,[18a] 8-bromo-2′,3′-*O*-isopropylideneadenosine,[18b] and cytidine-2′,3′-cyclic phosphate (sodium salt[18c]), respectively.

NMR Spectroscopy. Nucleosides **1–8** were studied with ^1H NMR spectroscopy at 500 MHz. The full set of ^1H NMR spectral parameters (chemical shifts and J-couplings) is summarized in Table IV. The calculated relative populations of the rotamers γ^+, γ^t, and γ^- around the C4′–C5′ bond are also given.[21] The data in Table IV reveal that nucleosides **1–4**, which have exo orientation of the 2′,3′-fused three-membered ring, correspond to $J_{1',2'}$ and $J_{3',4'}$ coupling constants <0.5 Hz, thus indicating that all members of this subset have a highly comparable furanoid conformation. The small values of $J_{1',2'}$ and $J_{3',4'}$ indicate that the bond H1′–C1′ is approximately orthogonal with respect to H2′–C2′, and the same holds true for the bond H3′–C3′ with respect to H4′–C4′. Of course, no accurate calculation of the torsion angles H1′–C1′–C2′–H2′ and H3′–C4′–H4′ is possible, since the geometric distortions at C2′ and C3′ preclude direct application of a Karplus-type equation. The X-ray crystal structural data on the nucleosides **1** and **4** also show a near-orthogonal orientation of H1′–C1′ to H2′–C2′, and H3′–C3′ to H4′–C4′, which is due to a flat geometry of the furanose ring. Thus, it is likely that the same conformational preference exists both in the solid state and in solution. Furthermore, appreciable differences are noted for the coupling constant $J_{2',3'}$ in **1–4**. Most likely, the different values for $J_{2',3'}$ must be ascribed

---

(20) Westhof, E.; Sundaralingham, M. *J. Am. Chem. Soc.* **1980**, *102*, 2534.

(21) Haasnoot, C. A. G.; de Leeuw, F. A. A. M.; de Leeuw, H. P. M.; Altona, C. *Recl. Trav. Chim. Pays-Bas* **1979**, *98*, 576.

Table IV. ^{1}H NMR (500 MHz) Spectral Data (δ in ppm relative to TMS, J in Hz) and Calculated Relative Populations (%) of the Staggered C4′–C5′ Rotamers $\gamma(+)$, γ(trans), and $\gamma(-)$

compd	$\delta 1'$	$\delta 2'$	$\delta 3'$	$\delta 4'$	$\delta 5'$	$\delta 5''$	$J_{1',2'}$	$J_{2',3'}$	$J_{3',4'}$	$J_{4',5'}$	$J_{4',5''}$	solvent	$x(\gamma(+))$	$x(\gamma(\text{trans}))$	$x(\gamma(-))$
1	5.98	1.94	1.94	4.13	3.68	3.61	<0.5	6.4	<0.5	4.1	5.6	*a*	55	35	15
2	5.91	3.15	3.25	4.16	3.69	3.70	<0.5	4.2	<0.5	5.1	4.6	*b*	40	38	22
3	5.50	3.86	3.75	4.30	3.63	3.62	<0.5	5.9	<0.5	4.8	4.8	*c*	39	38	23
4	6.21	4.46	4.22	4.18	3.58	3.50	<0.5	2.7	<0.5	5.4	5.1	*d*	32	41	27
5	6.11	3.74	3.58	4.28	3.68	3.65	2.3	5.0	2.5	6.3	5.7	*c*	24	45	31
6	6.20	3.98	3.93	4.20	3.96	3.95	<0.5	3.1	<0.5	5.4	6.5	*c*	30	38	22
7	6.19	3.85	3.62	4.30	3.69	3.65	<0.5	3.0	<0.5	5.5	6.1	*c*	28	41	31
8	6.20	3.83	3.60	4.24	3.71	3.65	<0.5	3.0	<0.5	5.5	6.1	*c*	28	41	31

[a] $CDCl_3$–CD_3OD (9:1). [b] D_2O–CD_3OD (9:1). [c] D_2O. [d] $(CD_3)_2SO$.

to the distinct electronegativities of the atoms linked to C2′ and C3′ and slightly different bond angles within the three-membered ring, rather than to structural differences of the furanose rings. Noteworthy, $J_{2',3'}$ *decreases* in the order **1** (6.4 Hz) > **3** (5.9 Hz) > **2** (4.2 Hz) > **4** (2.7 Hz), which roughly parallels an *increase* in Huggins' electronegativity[22] for the atom directly attached to C2′ and C3′: 2.60 for C(H_2) in **1**, 2.60 for S in **3**, 3.05 for NH in **2**, and 3.50 for O in **4**. The structures of nucleosides **5**–**8**, in which the 2′,3′-fused three-membered ring is on the endo face of the furanose ring, also show small $J_{1',2'}$ and $J_{3',4'}$ values (Table IV). While **6**–**8** again show $J_{1',2'}$ and $J_{3',4'}$ values <0.5 Hz, it is found for **5** that $J_{1',2'} = 2.3$ Hz and $J_{3',4'} = 2.5$ Hz. A priori, it is difficult to translate the small $J_{1',2'}$ and $J_{3',4'}$ values for **5**–**8** into an apparently preferred furanose conformation. At this point, however, we can turn to Krayevski's analysis of compound **8** which adopts a *puckered* O(4′)-endo furanose ring.[17] This conformation again corresponds to an approximately orthogonal orientation of H1′–C1′ with respect to H2′–C2′ and H3′–C3′ with respect to H4′–C4′ (vide infra); i.e., a very similar puckered furanose conformation is likely to exist also in solution. On the basis of all these data, we anticipate that the furanoid conformations in **6**–**8** in solution all closely resemble the crystal structures **8a** and **8b**. Most probably, the furanoid ring in **5** is puckered to a lesser extent, possibly because of steric crowding between the relatively bulky sulfur atom and the base moiety. This idea is corroborated by molecular mechanics calculations on structure **5** (vide infra).

Two additional remarks conclude the description of our NMR analyses on **1**–**8**. I: For compounds **4**, **6**, **7**, and **8**, which are relatively stable structures, we also measured 500-MHz ^{1}H NMR spectra at 65 °C. These experiments showed *no* apparent changes in the J coupling constants $J_{1',2'}$, $J_{2',3'}$, and $J_{3',4'}$ upon increasing the sample temperature. This strongly indicates that the furanose ring is not involved in a conformational equilibrium in solution, but instead adopts one unique conformation. II: It may be noted that $J_{1',2'}$ approximately equals $J_{3',4'}$ for each of the compounds **1**–**8**. This implies that the torsion angles H2′–C2′–C1′–H1′ and H2′–C2′–C1′–H1′ have the same absolute magnitude, at least to a good approximation. Alternatively stated, this means that the furanose moieties in **1**–**4** and **5**–**7** each adopt a conformation which is close to symmetric with respect to the plane through O4′, the atom in the "point" of the fused tricycle and the middle point of the bond C2′–C3′. It is of interest to note that this NMR-derived conclusion is strongly supported by the available X-ray structural data on the compounds **1**, **4**, and **8**.

Molecular Mechanics Calculations. The rather limited structural information that could be obtained from the ^{1}H NMR spectra of **1**–**8** has prompted us to use a computational approach for further structural studies. The MM2-87 molecular mechanics program, as provided in the CHEM3D package, was chosen.[23,24] Three points were considered in constructing starting geometries: (i) conformation of the sugar ring; (ii) conformation around the C4′–C5′ (γ) bond; (iii) conformation around the C1′–N1(9) (χ) glycosidic bond. Ad (i): calculations on **1**–**4** were started from a flat sugar ring. This was based on the crystal structures of **1** and **4**, and the observed analogy in the J couplings $J_{1',2'}$ and $J_{3',4'}$ in this subset (vide supra). Calculations on **5**–**8** were started from an O4′-endo puckered sugar ring, as found in the crystal structure of **8**. Calculations on **5** were also started from this sugar geometry, despite the fact that $J_{1',2'}$ and $J_{3',4'}$ differ for **5**, and **6**–**8** (Table IV). Ad (ii) and (iii): For each of the structures **1**–**8** we performed two series of 24 calculations. In the first series, the C4′–C5′ bond was placed in the $\gamma(+)$ domain and the base was rotated in 15° steps around the glycosidic C1′–N1(9) bond, from $\chi = -180°$ to $\chi = 180°$. The second series differed only with respect to the C4′–C5′ conformation, which was then placed in γ(trans). Each series produced a rough energy profile for rotation around the glycosidic bond; four such profiles are shown in Figure 4. Figure 4A displays the energy profiles for γ(trans) (open squares) and $\gamma(+)$ (filled diamonds) in structure **1**. The global energy minimum is found in the γ(trans) domain at $\chi \approx -105°$ (anti). Figure 4B shows the energy profiles for γ(trans) (open squares) and $\gamma(+)$ (filled diamonds) in structure **4**. In this case, the global energy minimum is also found in the γ(trans) profile, at $\chi \approx -120°$.

The global energy minimum for structure **1** at $\chi \approx -105°$ is in very close agreement with the experimental value $\chi = -106.9(4)°$ (Table II). The γ(trans) energy profile for **1** in Figure 4A indicates that the region between $\chi \approx -210°$ and $\chi \approx -60°$ should be easily accessible with a destabilization <0.5 kcal/mol with respect to the energy minimum. The close correspondence between the experimental and calculated χ should be regarded as a favorable coincidence, since the experimental χ is almost certainly determined in part by intermolecular interactions such as hydrogen bonding and stacking. Another important point to note is that the sugar ring in all 48 calculated structures of **1** showed a puckering amplitude between 7 and 10°, and a phase angle around 90° (O4′-endo). The furanose conformation as encountered in the crystal structure is thus

---

(22) Huggins, M. L. *J. Am. Chem. Soc.* **1953**, *75*, 4123.

(23) The molecular modeling system Chem3D-plus (Version 3.0) was used throughout this work. See: *Chem3D*, Cambridge Scientific Computing, Inc., Cambridge, MA. The best source of information regarding the force-field parameters is: Burker, U.; Allinger, N. L. *Molecular Mechanics*; ACS Monograph No. 177, American Chemical Society: Washington DC, 1982.

(24) We have also performed semiempirical AM1 and PM3 calculations on structures **1**–**8**. It was found, however, these these methods predicted planar furanoid rings *in each case*. It may be concluded that the AM1 and PM3 methods do not properly reflect the intrinsic tendency and furanoid rings to adopt a puckered conformation. This conclusion was also based on independent AM1 and PM3 calculations on unmodified nucleoside structures (Sandström, A.; Koole, L. H.; Chattopadhyaya, J. Unpublished results).

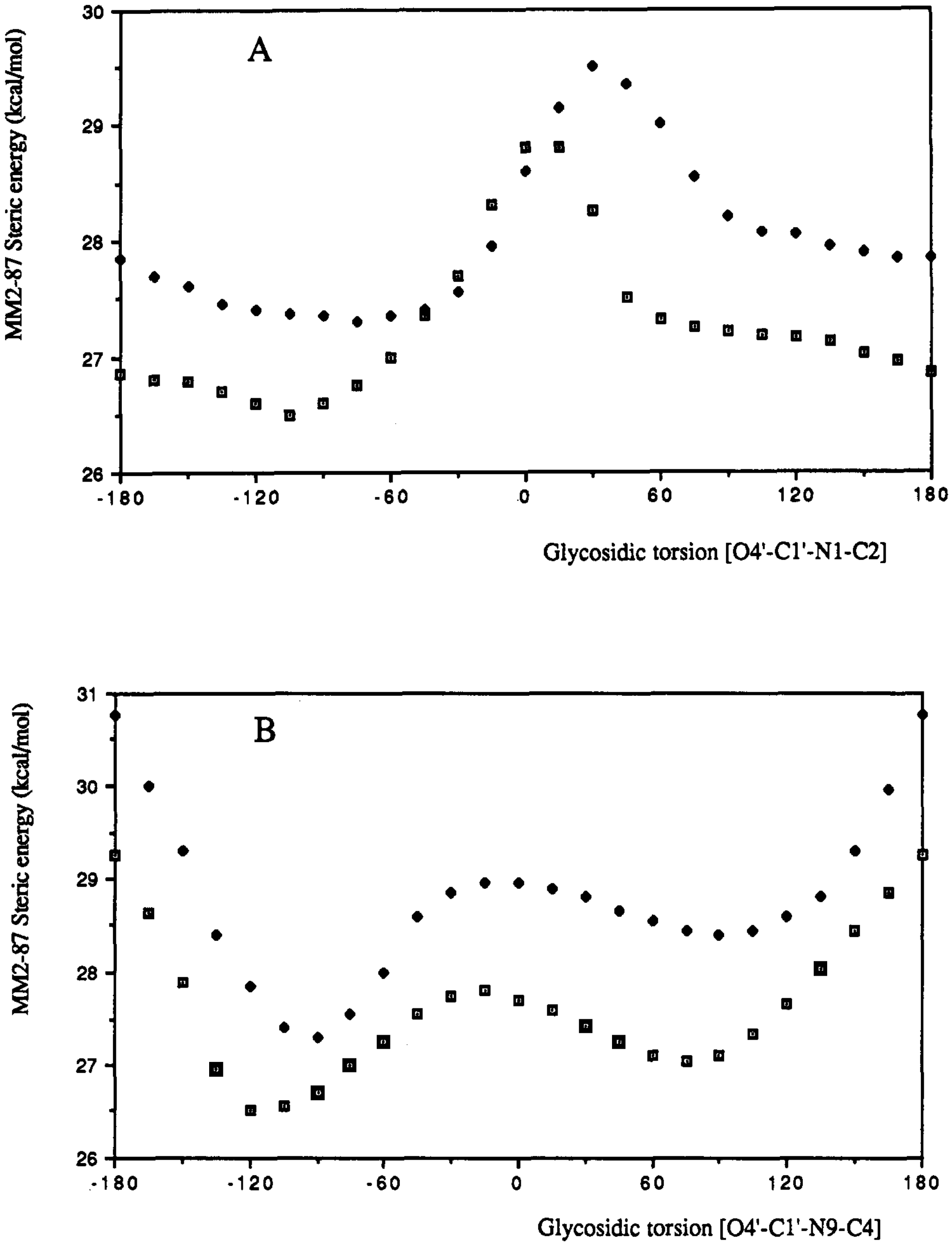

Figure 4. Energy profiles (MM2-87 calculations as in CHEM3D package) for rotation around the C1′–N glycosidic bond (15° steps) in structures 1 (graph A) and 4 (graph B). Open squares refer to γ(trans) conformation of the C4′–C5′ bond; filled diamonds correspond with γ(+) conformation around C4′–C5′ (see text).

accurately reproduced in our calculations. No indication for a correlation between the sugar conformation and χ was obtained. Most probably, the energy differences between the different sugar conformations are small relative to the stabilization/destabilization occurring upon rotation of the glycosidic bond (ΔE global maximum − ΔE global minimum ≈ 2.2 kcal/mol).

The calculations on structure 4 indicate to a global energy minimum at $\chi \approx -120°$ (anti), and γ(trans) conformation around C4′–C5′ (Figure 4B). Two next lowest minima were found, one at $\chi \approx 75°$ (syn) in the γ(trans) profile and one at $\chi \approx -90°$ (anti) in the γ(+) profile. The energy profiles for 4 in Figure 4 indicate that transition from anti to syn should be relatively facile; the energy barrier is predicted to be <2 kcal/mol. The glycosidic conformation with $\chi \approx 180°$ is a relatively high-energy maximum, due to eclipsing of C9–H9 and O4′ (≈2.6 kcal/mol destabilization relative to the global minimum). The crystal structures **4a** and **4b** show $\chi = -170.1$ (4)° (anti) and $\chi = 56.8$ (4)°, respectively, while both structures have the C4′–C5′ bond in γ(+). These data show that γ is wrongly predicted, and χ is accurately predicted for the syn orientation of the base, but not for the anti orientation. Most likely, these discrepancies are again due to the fact that intermolecular interactions in the crystal have an impact on the γ and χ conformations (vide supra). It is of importance to note that the sugar conformations in all 48 calculated structures of 4 had a puckering amplitude between 8 and 12° and a phase angle between 88° and 126°. As in the calculations on structure 1, there was no indication for a correlation between the sugar conformation and χ. Most likely, energy differences between the different sugar conformations are small relative to stabilization/destabilization which is associated with rotation of the base around the glycosidic bond. The calculations suggest that intermolecular interactions in the crystal do not have a major impact on the extent of puckering of the sugar ring (puckering amplitude), while they can tune the mode of puckering (phase angle), the glycosidic conformation, and the C4′–C5′ conformation in order to optimize

Table V. Results of the MM2-87 Calculations on Structures 1–8 (the Data Refer to the Global Energy Minima (See Text). Crystal Structural Data on 1, 4, and 8 Are Included for Comparison)

structure	glycosidic torsion [C2(4)–N1(9)–C1′–O4′]	steric energy (kcal)	phase angle (*P*)	puckering amplitude (ν_m)	torsion γ [O5′–C5′–C4′–C3′]
1	−105	26.5	91	10	−178
X-ray on **1**	−106.9 (4)	28.4[a]	86.7	8.8	−174.7 (4)
2	−105	24.7	83	8	180
3	−105	22.7	90	7	184
4	−120	26.3	90	11	206
X-ray on **4**					
4a (syn)	56.8 (4)	30.4[a]	123.0	8.1	42.9 (4)
4b (anti)	−170.1 (4)	27.6[a]	249.8	9.3	44.0 (4)
5	−165	32.0	88	24	183
6	−135	24.4	89	36	180
7	−135	26.3	89	35	181
8	−120	23.6	90	32	182
X-ray on **8**[17]					
A (anti)	−121.9 (4)	25.8[a]	98.9	29.2	−167.7 (4)
B (high syn)	121.2 (4)	26.6[a]	97.6	33.1	−177.5 (4)

[a] These steric energies were obtained after optimization of the bond lengths and bond angles as found in the crystal structures. The torsion angles were kept fixed at the experimental values during these minimizations.

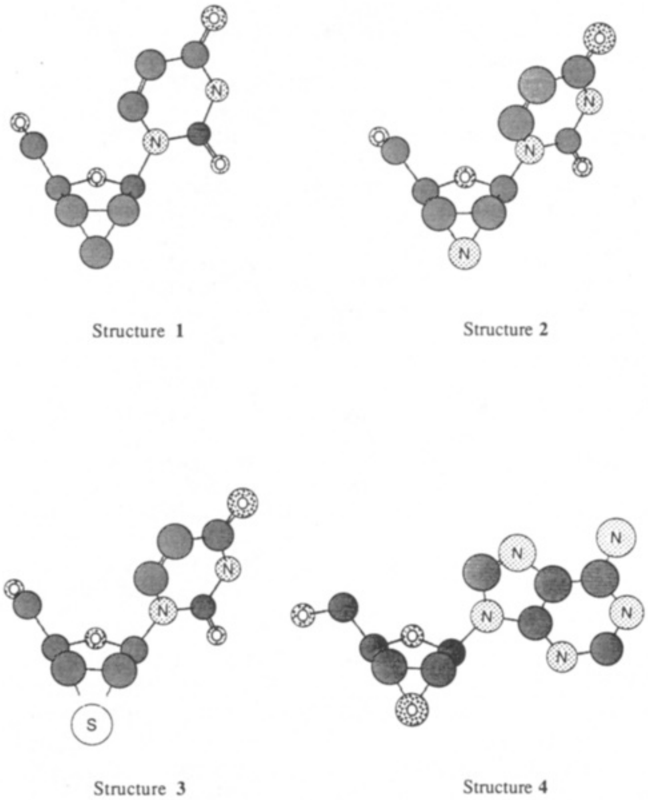

Structure 1

Structure 2

Structure 3

Structure 4

Figure 5. Lowest energy conformations (MM2-87 calculations as in CHEM3D package) of structures **1–4**. Geometric data are compiled in Table V. Note the overall similarity in these structures. For **4**, it was found that the combination (anti, γ-(trans)) (as shown in Figure 4) is more stable than (anti, γ(+)), (syn, γ(trans)), and (syn γ(+)). Note that the two conformations encountered in the crystal structure are (syn, γ(+)) (**4a**, viz. Figure 2) and (anti, γ(+)) (**4b**, viz. Figure 2).

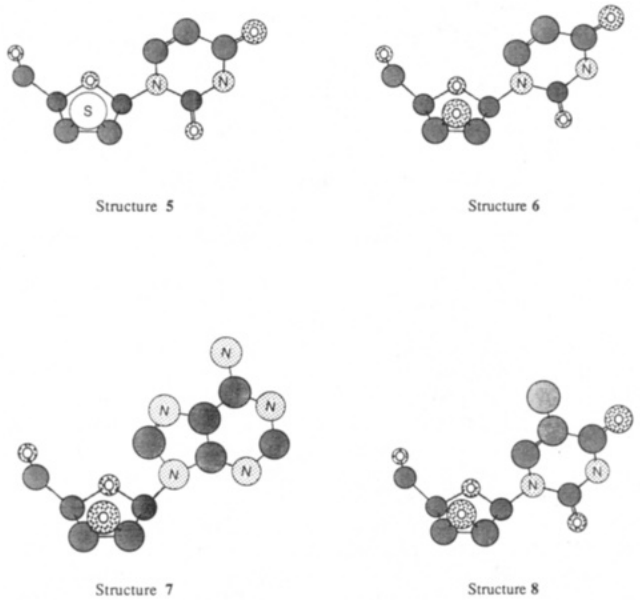

Structure 5

Structure 6

Structure 7

Structure 8

Figure 6. Lowest energy conformations (MM2-87 calculations as in CHEM3D packae) of structures **5–8**. Geometric data are compiled in Table V. Structures **6–8** are very similar. The furanose ring in structure **5** is less puckered in comparison with **6–8**. This result correlates with NMR spectroscopic data (see text).

hydrogen bonding and stacking interactions.

While the calculational results on structures **1** and **4** show that molecular mechanics should be used with extreme care, we performed analogous calculations on structures **2**, **3**, and **5–8**, which show a close structural similarity to **1** and **4**. Analogous energy profiles were obtained for structures **2**, **3**, and **5–8**. Glycosidic rotation of uracil or thymine typically led to one energy minimum in the anti range, whereas rotation of adenine produced two energy minima, one in the anti domain, and one in the syn domain. Table V compiles some characteristic conformational features of the lowest energy conformations of **1–8**; data on the crystal structures of **1**, **4**, and **8** were included to facilitate comparisons. Table V also contains the calculated steric energies for the crystal structures of **1**, **4**, and **8** (nonoptimized geometries). Figures 5 and 6 show the most favorable conformations of **1–8**. Several remarks can be made on the basis of the data in Table V: the optimized structures **2** and **3** show preferential anti orientation of the uracil base and a nearly flat geometry of the furanoid ring with slight O4′-endo puckering. These findings closely parallel the experimental and calculated data on **1** and **4**. Structures **6–8** show preferential anti orientation of the base, along with a substantially puckered furanoid ring, which is in line with the crystal structure of **8**. Syn orientation for the adenine base in **7** is predicted to cause a destabilization of almost 3 kcal/mol, in comparison with anti orientation. Calculations on structure **5** predict a less puckered furanoid ring (ν_m = 24°). Structure **5** may be regarded as an intermediate between the puckered structures **6–8** and the flat structures **1–4**. Most likely, this can be attributed to steric crowding on the β-face of the furanoid ring in **5**. This crowding involves the uracil base, the CH_2OH group, and the relatively bulky sulfur atom.

Concluding Remarks

Our present study has provided new detailed information about the structural properties of [3.1.0]-fused 2′,3′-modified nucleosides. The crystal structures of **1** and **4** show the following: (i) a virtually planar furanoid ring; (ii) expansion of the endocyclic bond angles C1′–C2′–C3′ and C2′–C3′–C4′ by 6–7°; (iii) shortening of the bonds C1′–C2′ and C2′–C3′ by ca. 0.03 Å. Conclusions ii and iii refer to comparison with the crystal structures of the native nucleosides. NMR data show conformational analogies in the series **1**–**4** on one hand and **6**–**8** on the other hand. Preliminary conclusions from J coupling data are as follows: (i) the furanoid rings in **1** and **4** adopt a planar conformation in solution, i.e., the crystal structure seems to be retained in solution; (ii) there is a close analogy between the conformational properties of **1**, **4** and **2**, **3**; (iii) structures **6**–**8** adopt a substantially puckered furanoid conformation (O4′-endo), as is also the case in the crystal structure of **8**; (iv) the furanoid ring in **5** is less puckered in comparison with **6**–**8**. Interestingly, these observations are reproduced by simple molecular mechanics calculations in which the molecular steric energy is calculated as a function of the glycosidic torsion angle χ. The calculated values for χ, however, may deviate from the values in the crystal structure, possibly as a consequence of the fact that intermolecular interactions have an important impact on χ.

Experimental Section

X-ray Crystallography. Structure of Compound 1. A colorless prismatic crystal of **1** having approximate dimensions of 0.15 × 0.05 × 0.06 mm was mounted on a glass fiber with its long axis roughly perpendicular to the ϕ-axis of the diffractometer. Preliminary examination and subsequent data collection were performed on an Enraf-Nonius Turbo CAD4 diffractometer–rotation anode system with graphite-monochromated CuK_α radiation (λ = 1.540 56 Å). Cell constants were obtained by least-squares refinement of 25 reflections in the range $11° < \theta < 29°$. They were: a = 8.110 (1) Å, b = 8.386 (2) Å, c = 15.038 (1) Å, in an orthorhombic unit cell. The subsequent analysis confirmed the space group to be $P2,2,2,$. Intensity data were collected at 23 °C with an $\omega/2\theta$ scan technique, a variable scan rate of 1–7° min^{-1} (in Ω), and a maximum scan time of 60 s per reflection. Data were collected in the range $1.5 < \theta < 67°$ with $0 \le h \le 9$, $0 \le k \le 10$, and $0 \le 1 \le 17$. A total of 1698 reflections was measured, which were merged to 1577 unique reflections. The agreement factors for the averaging of the nonunique reflections were 1.9% based on intensity and 1.4% based on F_0. A total of 1507 reflections had significant intensity with $I > 3\sigma(I)$ and were used in the subsequent refinements. A periodic check on the intensities of the three standard reflections during the data collection showed no statistically-significant crystal decay (<0.5%).

The structure was solved by routine application of direct methods,[25] with the most consistent E map showing all non-hydrogen atoms. The structure was refined by full-matrix least squares on F. The positions of all hydrogen atoms were found in difference Fourier maps and these, together with hydrogen atom isotropic thermal parameters, were included in the latter cycles of refinement. Refinement converged to an R of 0.036 and R_w of 0.034 with weights of the form $w = 1/[\sigma^2(F) + 0.04(F)^2]$. The maximum Δ/σ in the final least-squares cycle was 0.1 and the esd of an observation of unit was 0.79. The final difference Fourier map had maximum and minimum electron density levels of ±0.25 e $Å^{-3}$. An empirical absorption correction[26] was applied prior to the final refinements. Tables of temperature factors have been deposited. Coordinates are listed in Table I. Atomic scattering factors were taken from International Tables for X-ray Crystallography.[27] Calculations were performed with the SDP package.[28]

Structure of Compound **4**. Crystals of **4** were grown from a saturated solution in methanol by slowly evaporating the solvent at an ambient temperature. The space group was $P1$, and the unit cell parameters were as follows: a = 4.834 (1) Å, b = 6.893 (1) Å, c = 15.942 (2) Å; α = 90.51 (1)°, β = 97.16 (2)°, γ = 89.27 (2)°; V = 527.1 $Å^3$; Z = 2. The unit cell contains two crystallographically independent molecules. The parameters of the unit cell and the intensities of reflections were measured with a CAD-4F diffractometer, using the ω/θ scan technique, CuK_α radiation, and a graphite monochromator. A full reciprocal sphere was measured, and the intensities of reflections were averaged in order to reduce possible experimental errors. The intensities of 1376 independent reflections with $I > 3\sigma(I)$ were used in the work. The experimental data were collected for the Lorenz and polarization factors. The structure was determined by direct methods and refined by full-matrix least-squares analysis with anisotropic temperature factors for C, N, and O atoms. The positions of H atoms were located on difference Fourier maps and refined in isotropic approximation. Tables of temperature factors have been deposited. Coordinates are listed in Table IV. The refinement converged at R = 4.1%. All calculations were made with the SDP package.[28]

NMR Spectroscopy. The ^1H NMR spectra were recorded on a Bruker AMX 500 NMR spectrometer, interfaced with an X-32 computer system. Sample concentrations were in the range 15–25 mM. Chemical shifts were referenced against a trace of internal reference, which was acetonitrile (δ 2.00 ppm) for the aqueous samples and tetramethylsilane (δ 0.00 ppm) in the case of an organic solvent (mixture). All ^1H NMR spectra were run in the FT mode, using a sweep width of 5000 Hz, and a time domain of 32k. After zero-filling to 64k, the free-induction decays were apodized with a Gaussian window in order to enhance the resolution. The J coupling constants as summarized in Table IV could be determined with an accuracy of ±0.1 Hz. For some non-first-order subspectra, a routine NMR-spectrum simulation algorithm was used to obtain accurate J couplings and chemical shifts.

Acknowledgment. We thank the Swedish Board for Technical Development (STU), the Swedish Natural Science Research Council (NFR), Wallenbergstiftelsen, Swedish Research Council (FRN); Medivir AB (Huddinge, Sweden) and University of Uppsala for financial support (to J.C.). We also thank the Cancer Research Campaign in the United Kingdom for generous financial support (to S.N.). Financial support from the European Molecular Biology Organization (EMBO) through a two-year fellowship to L.H.K. is greatfully acknowledged.

Registry No. 1, 129779-53-9; 2, 125418-18-0; 3, 63244-59-7; 4, 2627-64-7; 5, 63244-55-3; 6, 14042-38-7; 7, 40110-98-3; 8, 14486-22-7.

---

[25] Main, P.; Fiske, S. J.; Hull, S. E.; Lessinger, L.; Germain, G.; DeClercq, J.-P.; Woolfson, M. M. MULTAN82; Universities of York, England, and Louvain, Belgium.

[26] Walker, N.; Stuart, D. *Acta Crystallogr., Sect. A* **1983**, *A39*, 158.

[27] *International Tables for X-ray Crystallography*; Kynoch Press: Birmingham, England, 1974; Vol. 4, pp 99–100.

[28] *Enraf-Nonius Structure Determination Package*; Enraf-Nonius: Delft, Holland; B. A. Frenz and Associates: College Station, TX, 1986.